# The Conformational Landscape of *m*-Anisic Acid and its Complexes with Formic Acid.

*Alberto Macario,*[a] *Susana Blanco,*[a]* *Javix Thomas,*[b] *Yunjie Xu,*[b] *Juan Carlos López*[a]*

[a] Dpto. Química Física y Química Inorgánica, Facultad de Ciencias, IU Cinquima, Universidad de Valladolid, Paseo Belén 7, 47011-Valladolid, SPAIN.

[b] Department of Chemistry, University of Alberta, Edmonton, Alberta, Canada, T6G 2G2

## ABSTRACT

Four conformers of *m*-anisic acid were observed in a supersonic expansion using Fourier transform microwave spectroscopy. These conformers correspond to different relative orientations of the acid and the methoxy groups and have their planar skeletons stabilized by resonance. When formic acid was present in the jet, the spectra of four *m*-anisic acid–formic acid heterodimer conformers were detected. The complexes are formed from the interaction of formic acid with each of the four observed conformers of *m*-anisic acid through the typical acid-acid sequential cycle with a double O-H···O=C hydrogen bond interaction in a pseudo eight-membered ring arrangement. The four heterodimer forms retain the same four *m*-anisic acid conformational geometries and the same relative abundances of the *m*-anisic acid monomeric forms in the supersonic expansion. This proves that a kinetic mechanism dominates the formation of complexes in the jet.

## INTRODUCTION

The medical benefits of the anise seed (*Pimpinella anisum*) are known since the antiquity. As a traditional herbal medicine, anise has been mainly employed by its carminative effect. Anisic acids (*o*-, *m*- and *p*-methoxybenzoic acids, AA) are minority components of the anise seed, but present a wide range of biological activities that can be related with the pharmaceutical properties of this herb. They may act as inhibitors of bacterial growth[1] and in different enzymatic processes.[2] For example, AAs act as allosteric inhibitors of the isocitrate lyase (ICL) enzymatic activity.[3] In some cases, the relative position of the substituents in the aromatic ring influences the role that these acids play in catalytic processes. For instance, *o*-AA increases the enzyme and specific activity of catalase, while *m*-AA and *p*-AA isomers produce the opposite effect.[3]

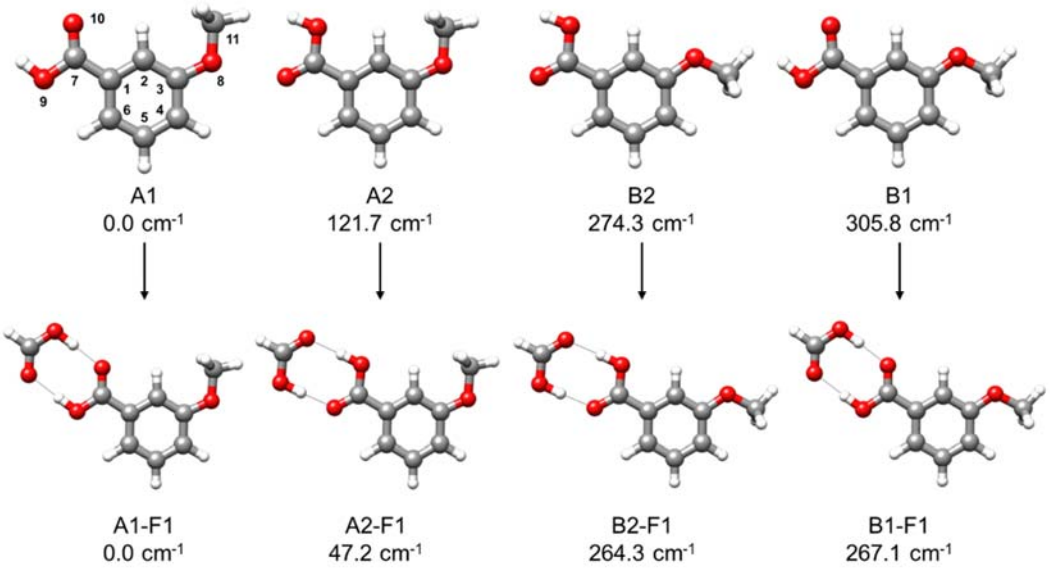


Figure 1. Low energy forms of *m*-anisic acid (*m*AA) monomer and *m*-anisic acid – formic acid (*m*AA-FA) heterodimer and their B3LYP-D3/6-311++G(d,p) energies relative to the global minima.

Moreover, *m*-AA (3-methoxybenzoic acid) is also employed as a food flavoring ingredient.[4] It appears that there is a direct relation between the chemical and biological properties of AAs and their molecular structures.

One of the functional groups of *m*-AA is the carboxylic group. This group appears very frequent in biomolecules, for example, amino acids and nucleic acids. Its capacity of acting as a double hydrogen bond donor/acceptor makes it one of the most important interaction sites in biological systems. Moreover, it forms easily dimers or heterodimers with other acids adopting an eight-membered ring structure through a double O-H···O hydrogen bond. These hydrogen bonds are usually considered to be very strong due to the additional stabilization of resonance-assisted hydrogen bond (RAHB).[5] This acid-acid interaction has been taken as a prototype for the doubly hydrogen bonded DNA base pairs which control the transcription and translation

processes of the genetic information.[6] Moreover, this interaction is associated with the double proton transfer when it connects two equivalent dimer forms.[7] Proton transfer has been related to the possible appearance of genetic mutations of DNA.[8-10] The first microwave spectroscopic study of an acid-acid heterodimer was done by Costain and Srivastava at room temperature in 1961.[11] Since then, different works on this subject have been done.[7,8,12-21] The most recent ones focused on the proton transfer process,[7,8,14-17] or on the study of conformational equilibria.[18-21] The systems for which the highest number of different acid-acid complex conformations have been observed are acrylic acid-difluoroacetic acid cluster[7] and *o*-AA-FA complex[21] with four conformers in each case. The most interesting aspect of the last system is the observation of two forms of the complex with *o*-AA bearing a *trans*-COOH arrangement, the first time that such uncommon complex structures were observed.

A previous study of the *o*-, *m*- and *p*-anisates of lithium, sodium and potassium using FT-IR, FT-Raman and $^{1}$H NMR spectroscopy methods[22] was done assuming that AA adopts only B2 form (see Figure 1). On the other hand, a combined IR, $^{13}$C and $^{1}$H NMR work of *m*-AA[23] in solution only considered the two possible orientations of the methoxy group to conclude that A form is more stable than B form with relative abundances of A:B = 3:1.

Rotational spectroscopy has been extensively employed as one of the reference techniques to determine the molecular structure of molecules and clusters in the gas phase.[24] We have recently used this technique to investigate the molecular structure and the conformational equilibria of *o*-AA[25] and its complexes with water[25] or formic acid (FA).[21] The structure of *o*-AA[25] is mainly governed by the intramolecular interactions between its functional groups giving rise to three different conformers. In one of them, T1, a strong O-H···O intramolecular hydrogen bond is established from the acid group to the methoxy group, resulting in a *trans*-COOH arrangement.

In the other two conformers, C1 and C2, the acid group is in the standard *cis*-COOH disposition and the interactions between the acid and the methoxy group are repulsive. In the C1 and C2 forms, which correspond to the two possible relative orientations of the COOH group, the repulsion induces a small torsion of the COOH group with respect to the aromatic ring plane. In the present work, we extend this study to *m*-AA with the aim of investigating the forces that rule its conformation and molecular structure. In this case, the acid and methoxy groups are far apart precluding the formation of intramolecular hydrogen bonds between them. Resonance between the aromatic ring and the substituents is expected to be the dominating force thus stabilizing a planar skeleton structure. In this way the four possible conformers A1, A2, B1 and B2 shown in Figure 1 could be regarded as the combinations of the two possible orientations of the methoxy (A or B) and the carboxylic groups (1 or 2).

In this work we present a study of the molecular structure and conformational landscape of *m*-AA and its complex with FA. We have used rotational spectroscopy to analyze the low energy conformers of *m*-AA in the gas phase, their relative stability and the possible alteration of this equilibrium by complexation with FA. This study will allow a better understanding of the structure of these systems and, consequently, of their chemical properties which in turn govern their biological activities. The results are compared to those recently obtained for *o*-AA[25] and its heterodimers with FA.[21] One interesting aspect of this research is to analyze how the configuration of the substituents affects to the ring structure. It is known that the presence of non-symmetric substituents in the phenyl ring with respect to the substitution axis causes an imbalance between the two principal canonical structures of the aromatic ring, favoring one form against the other. This effect, known as Angular-Group Induced Bond Alternation (AGIBA),[26,27] is also taken into account in this work.

## METHODS

### Experimental methods

Commercial samples of *m*-AA and FA were used without further purification. The rotational spectra have been recorded using broadband chirped-pulse Fourier transform microwave (CP-FTMW) spectrometers[28] in the Universities of Alberta (7-18 GHz)[29] and Valladolid (2-8 GHz).[30] The carrier gases employed were He, Ne and Ar at stagnation pressures of 1-4 bar. For the cluster formation, the FA was previously mixed (<0.5%) with the carrier gas. *m*-AA (m. p. ~ 98-100 ºC, b. p. ~ 200ºC) was placed in the nozzle reservoir and heated at around 135ºC. The resulting gas mixture was expanded through a nozzle of 0.8 mm inside the chamber to form a supersonic jet where the molecular clusters were formed. The length of the molecular pulses ranges from 700 to 900 μs duration depending of the carrier gas used. In the CP-FTMW of Valladolid, chirp pulses of 5 μs were created by an arbitrary waveform generator and amplified to 20 W. The polarization radiation power poses a limit of *ca.* 2 GHz in the exploration bandwidth so the complete spectrum (2-8 GHz) was recorded in three steps. The polarization signal was radiated from a horn antenna in a direction perpendicular to that of the expanding gas. A molecular transient emission spanning 40 μs is then detected through a second horn, recorded with a digital oscilloscope and Fourier-transformed to the frequency domain. The estimated accuracy of the frequency measurements is better than 15 kHz. The CP-FTMW spectrometer at the University of Alberta has a similar design[29] with some minor differences. An arbitrary waveform generator is used to generate a 4 μs long pulse with a frequency chirp from 0 to 1 GHz. This chirped pulse is then mixed with the output of a MW synthesizer to produce a 2 GHz

MW chirped pulse which is amplified by a 20 W solid state MW amplifier and then propagated into the vacuum chamber using a wide-band, high-gain MW horn antenna.

Complementary measurements were done in the University of Alberta on a cavity molecular beam Fourier transform microwave spectrometer (MB-FTMW) working in the 8-18GHz frequency region.[31,32] In this instrument, the sample was held in a stainless-steel reservoir right behind a General Valve nozzle and neon gas at backing pressures of 2-4 bar was flowed over the sample to bring a trace amount of *m*-AA into the sample cavity. Each line is split into two Doppler components because the orientation of the supersonic jet expansion is collinear with the resonator axis. The rest frequency was calculated as the arithmetic mean of the frequencies of the Doppler components. The estimated accuracy of the frequency measurements using this instrument is better than 2 kHz.

**Computational methods**

A conformational search has been done at the B3LYP-D3/6-311++G(d,p) level of theory to explore the potential energy surface (PES) of *m*-AA and its complexes with FA. Four stable conformers of the monomer were found (see Figure 1). Their predicted rotational parameters are collected in Table 1. The conformers are labelled to indicate the relative arrangement of the methoxy and carboxyl groups. The first label, A or B, refers respectively to the *cis* or *trans* disposition of the methyl group with respect to the hydrogen atom in *ortho* position with respect to both functional groups. The second label, 1 or 2, refers to the orientation of the COOH group to describe whether the CO or the OH groups, respectively, is next to the same *ortho* H atom. No conformer in *trans* configuration for the COOH group were found to be stable, in contrast to the case of *o*-AA. For the *m*-AA – FA cluster, up to nine different conformers were found (Figure S2 and Table S1 of supporting information). The four most stable species, which keep the same *m*-

AA structures of the four monomer conformations, are shown in Figure 1 and their predicted rotational parameters are listed in Table 1. Complementary *ab initio* calculations at the MP2/ 6-311++G(d,p) and MP2/aug-cc-pVDZ levels of theory were employed to predict the dissociation energies, to explore the PES minimum energy pathways to conformer interconversion and to calculate the Gibbs energies to estimate the relative conformational abundances. The dissociation energies were corrected for basis set superposition error (BSSE) using the counterpoise method.[33] These were calculated at the MP2/6-311++G(d,p) level in order to have values comparable to those of related complexes previously reported. All the calculations were done using the Gaussian 09 program package.[34]

Table 1. Spectroscopic parameters predicted at the B3LYP-D3/6-311++G(d,p) level of theory for the four most stable conformers of *m*-anisic acid (*m*-AA) and *m*-anisic acid – formic acid (*m*-AA – FA) heterodimer.

| ***m*-AA** | **A1** | **A2** | **B2** | **B1** |
|---|---|---|---|---|
| ***A*/MHz** [a] | 1901.03 | 1859.36 | 2445.46 | 2505.39 |
| ***B*/MHz** | 775.73 | 788.21 | 665.45 | 657.43 |
| ***C*/MHz** | 552.86 | 555.51 | 524.86 | 522.52 |
| $P_{cc}$/uÅ$^2$ | 1.61 | 1.61 | 1.61 | 1.61 |
| $\mu_a$/D | -0.6 | 2.0 | -3.3 | -2.3 |
| $\mu_b$/D | 0.6 | -1.7 | -0.1 | 2.5 |
| $\mu_c$/D | 0.0 | 0.0 | 0.0 | 0.0 |
| $\Delta E_{DFT}$/cm$^{-1}$ | 0.0[c] | 121.7 | 274.3 | 305.8 |
| $\Delta G_{418K}$[b]/cm$^{-1}$ | 0.0[d] | 79.0 | 231.1 | 253.7 |
| ***m*-AA – FA** | **A1-F1** | **A2-F1** | **B2-F1** | **B1-F1** |
| ***A*/MHz** [a] | 1362.78 | 1451.53 | 1873.73 | 1733.08 |
| ***B*/MHz** | 300.64 | 293.10 | 262.94 | 268.39 |
| ***C*/MHz** | 246.69 | 244.24 | 230.92 | 232.92 |
| $P_{cc}$/uÅ$^2$ | 1.61 | 1.61 | 1.61 | 1.61 |
| $\mu_a$/D | 1.3 | 1.3 | 3.2 | -3.3 |
| $\mu_b$/D | 1.0 | -0.8 | 0.8 | 0.6 |
| $\mu_c$/D | 0.0 | 0.0 | 0.0 | 0.0 |
| $\Delta E_{DFT}$/cm$^{-1}$ | 0.0[e] | 47.2 | 264.3 | 267.1 |
| $\Delta G_{418K}$[b]/cm$^{-1}$ | 0.0[f] | 0.2 | 161.5 | 192.9 |

[a] *A*, *B* and *C* are the rotational constants. $P_{cc} = (I_a + I_b - I_c)/2$ is a planar moment of inertia. $\mu_a$, $\mu_b$ and $\mu_c$ are the components of the permanent electric dipole moment. $\Delta E$ is the electronic energy relative to conformer A1 for the monomer and A1-F1for the heterodimer. [b] $\Delta G$ is the Gibbs energy relative to that of the most stable form calculated at 418K and 2bar. [c] Absolute electronic energy is -535.5191934 $E_h$. [d] Absolute Gibbs energy is -535.426344 $E_h$. [e] Absolute electronic energy is -725.3771589 $E_h$. [f] Absolute Gibbs energy is -725.259868 $E_h$.

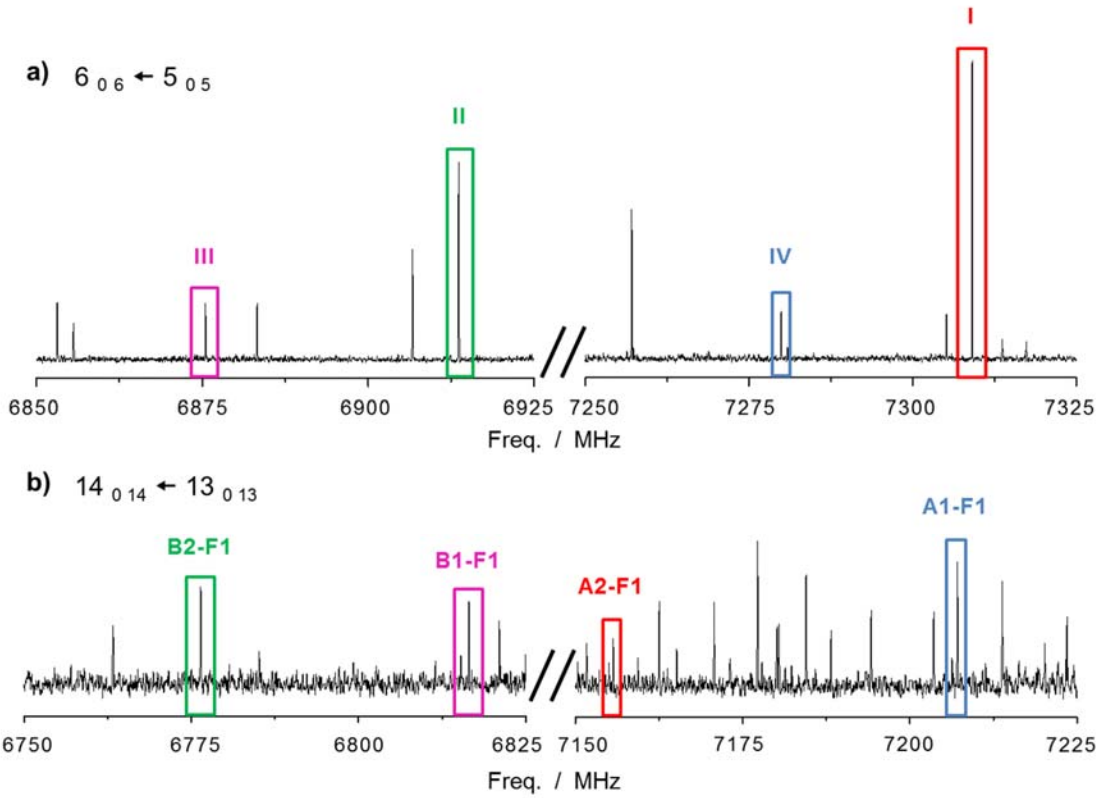


Figure 2. a) Sections of the spectrum of *m*-anisic acid (*m*-AA) showing the assignment of the $6_{0,6}$←$5_{0,5}$ transition for the species I (A2), II (B2), III (B1) and IV (A1). b) The spectrum of *m*-anisic acid – formic acid (*m*-AA-FA) showing the assignment of the $14_{0,14}$←$13_{0,13}$ transition to the conformers A1-F1, A2-F1, B1-F1 and B2-F1.

## RESULTS AND DISCUSSION

### Rotational Spectra

All *m*-AA predicted forms are prolate asymmetric tops and, with the exception of form A1, present a high value of the $\mu_a$ electric dipole component (Table 1). Initial assignment analysis of the spectrum was done on the 2-8 GHz CP-FTMW spectrum of the *m*-AA monomer (see Figures 2 and S3) by identifying the characteristic patterns of the $\mu_a$-type R-branch transitions which form well defined groups of J+1←J lines spaced *ca*. B+C. Additional assignments were later made in the 8-14 GHz frequency region. The initial survey led easily to the assignment of the

most intense lines of a species, labelled I (see Figure 2) for which 236 $\mu_a$- and $\mu_b$-type transitions of the R-, Q- and P-branches were measured. Removing those lines from the spectrum allows us to assign the second spectrum in order of decreasing intensity, labelled as II, for which a total of 61 $\mu_a$-type R-branch transitions were measured. Removing again those newly assigned lines, the transitions of two new weaker species showing similar intensities and labelled as III and IV were identified. For rotamer III, up to 116 $\mu_a$- and $\mu_b$-type lines belonging to the R- and Q-branches were observed. Finally, for species IV, 92 $\mu_a$- and $\mu_b$-type transitions of the R- and Q-branches were measured. All the spectra were analyzed using the Watson´s semirigid Hamiltonian[35] in the A reduction and the $I^r$ representation. The determined rotational parameters are reported in Table 2. No splittings attributable to the internal rotation of the methyl group were observed for any species, in agreement with other rotational studies of structurally similar molecules, such as anisole[36] or *o*-AA.[25]

The assignment of the observed species to plausible conformers of *m*-AA was done by comparing the predicted and experimental rotational parameters (see Tables 1 and 2). In addition, the electric dipole moment components can be related to the observed transition selection rules and the polarization power needed to optimally polarize the observed transitions using the MB-FTMW spectrometer. The observed rotamers can be classified into two groups according to the values of their rotational constants. Species I and IV have similar rotational constants which can be correlated with the predicted *m*-AA conformers labelled as A. In the same way, rotamers II and III can be correlated with the B forms. The non-observation of $\mu_b$-type transitions for species II identifies it as B2 conformer, with $\mu_b$ dipole moment component predicted to be close to zero. Thus, species III was subsequently assigned to B1. Both I and IV species show $\mu_a$- and $\mu_b$-type transitions. However, the relative low microwave power needed for

the optimum polarization of the $\mu_a$- and $\mu_b$-type transitions of species I allows one to correlate it with conformer A2 (see Table 1) which has moderately higher values of the predicted dipole moment components than A1. Hence, species IV that needs a high polarization power to polarize its $\mu_a$- and $\mu_b$-type transitions was assigned to A1. As one can see, the different orientation of the methoxy group causes noticeable shifts in the values of the rotational constants, and in addition the relative arrangement of the $CH_3$ and COOH groups leads to important changes in the values of the electric dipole moments.

Table 2. Experimental rotational parameters for the four observed conformers of *m*-anisic acid (*m*-AA).

| **Parameters**[a] | ***m*-AA IV (A1)** | ***m*-AA I (A2)** | ***m*-AA II (B2)** | ***m*-AA III (B1)** |
|---|---|---|---|---|
| ***A*/MHz** | 1903.02382(32)[b] | 1860.87923(11) | 2447.94910(78) | 2509.04470(27) |
| ***B*/MHz** | 779.83252(12) | 792.545106(51) | 668.14761(17) | 659.863398(93) |
| ***C*/MHz** | 555.44906(13) | 558.153185(40) | 526.99894(18) | 524.557697(89) |
| $P_{cc}$/uÅ$^2$ | 1.88532(18) | 1.899056(61) | 1.93142(29) | 1.93440(15) |
| $\Delta_J$/kHz | 0.0083(11) | 0.08760(94) | 0.0054(17) | 0.01082(48) |
| $\Delta_{JK}$/kHz | - | -0.2474(22) | - | -0.00557(39) |
| $\Delta_K$/kHz | - | 0.1664(15) | - | - |
| $\delta_J$/kHz | 0.01021(53) | -0.02569(39) | - | - |
| $\delta_K$/kHz | -0.00686(95) | 0.09371(91) | - | - |
| **N** | 92 | 236 | 61 | 116 |
| **σ/kHz** | 5.6 | 5.1 | 5.0 | 5.7 |

[a] *A*, *B* and *C* are the rotational constants. $P_{cc}=(I_a+I_b-I_c)/2$ is a planar moment of inertia. $\Delta_J$, $\Delta_{JK}$, $\Delta_K$, $\delta_J$ and $\delta_K$ are the quartic centrifugal distortion constants. N is the number of rotational transitions fitted. $\sigma$ is the rms deviations of the fit. [b] Standard error are given in parentheses in units of the last digits.

Once the assignment of *m*-AA was completed, the rotational spectrum of the mixture of *m*-AA and FA was recorded (see Figures 2 and S3). The tendency of FA[37] to dimerize[38] easily or to form aggregates with other molecules present in the mixture, such as water[39] or the carrier gas,[40] gives rise a high number of lines belonging to FA or its complexes in the observed spectrum. Consequently, all the known transitions of the FA species and of the four conformers of *m*-AA were removed from the CP-FTMW spectrum prior to the rotational assignment of the *m*-AA – FA complex. Following a similar search and assignment procedures as described above, four different species belonging to A1-F1, A2-F1, B1-F1 and B2-F1 conformers (see Figure 1 and Table 1) were identified. All the measured transitions were analyzed with the same Hamiltonian used for the monomer. The results are shown in Table 3. The assignment of the observed species to the predicted conformer of Table 1 is based in the good agreement between the observed and predicted rotational constants. There is also a good consistency between the predicted dipole moments and the selection rules observed and the microwave power needed to optimally polarize the different transitions of the heterodimer species.

**Conformational landscape and molecular structure**

The experimental values of the planar moment of inertia $P_{cc}$ ($P_{cc} = (\Sigma_i m_i c_i^2)/2$), which measures the mass extension out of the *ab* inertial plane, allow us to discuss the degree of planarity of the *m*-AA monomer and the *m*-AA – FA clusters. The $P_{cc}$ values for the *m*-AA conformers lie in the range 1.88-1.94 u·Å$^2$ (see Table 2), being similar to those observed for *o*-AA T1 form (1.97 u·Å$^2$)[25] or anisole (1.77 u·Å$^2$).[36] Such planar moments correspond to planar skeleton conformers where their only contributions are from the methyl group out-of-plane hydrogen atoms. For the four *m*-AA – FA complex conformers, $P_{cc}$ take values in the range 2.26-2.36 u·Å$^2$ (see Table 3). These values can be also attributed to planar skeleton structures of the observed complex

conformers if we take into account the possible contributions of out-of-plane intermolecular vibrations. This hypothesis is reasonable if we assume that the structures of the *m*-AA conformers do not changes (see Figure 1) upon complexation with FA, where all the complexes bear the same double hydrogen bond sequential cycle interaction.

Table 3. Spectroscopic parameters determined for the four observed conformers of the *m*-anisic acid – formic acid (*m*-AA – FA) heterodimer.

| **Parameters**[a] | **A1-F1** | **A2-F1** | **B2-F1** | **B1-F1** |
|---|---|---|---|---|
| ***A*/MHz** | 1375.51660(32)[b] | 1448.81139(59) | 1865.840(44) | 1752.457(35) |
| ***B*/MHz** | 301.70254(24) | 295.58629(23) | 264.88514(25) | 269.20991(24) |
| ***C*/MHz** | 247.98262(16) | 246.04923(24) | 232.46039(31) | 233.86435(30) |
| $P_{cc}$/uÅ$^2$ | 2.2696(14) | 2.2996(17) | 2.3664(55) | 2.3293(51) |
| $\Delta_J$/kHz | 0.00602(78) | 0.00480(65) | 0.00328(59) | 0.00281(58) |
| $\Delta_{JK}$/kHz | -0.0062(10) | - | - | - |
| $\Delta_K$/kHz | 0.00392(69) | - | - | - |
| **N** | 95 | 50 | 46 | 48 |
| **σ/kHz** | 6.7 | 6.8 | 6.4 | 6.2 |

[a] *A*, *B* and *C* are the rotational constants. $P_{cc} = ( I_a + I_b - I_c)/2$ is a planar moment of inertia. $\Delta_J$, $\Delta_{JK}$ and $\Delta_K$ are the quartic centrifugal distortion constants. N is the number of rotational transitions fitted. $\sigma$ is the rms deviations of the fit. [b] Standard error are given in parentheses in units of the last digits.

The predicted rotational constants for the *m*-AA monomer and the *m*-AA – FA complex conformations agree with the experimental values within less than 1% (see Tables 1-3). Therefore, the B3LYP-D3/6-311++G(d,p) $r_e$ predicted structures could be taken as reasonable estimations of the molecular geometries. The comparison of the $r_e$ geometrical parameters for the four *m*-AA monomer and *m*-AA – FA complex conformers is given respectively in Tables S2 and S3 of the supporting information. The ring structures are almost equal for the two A conformers and the same happens for the two B forms. This means that the ring structure is predicted to be practically independent of the orientation of the acid group. On the other hand, as shown in Figure 3, the ring C-C distances are slightly different depending on the orientation of the methoxy group. The A structures seem to reflect the AGIBA effect,[26,27] which stabilizes one resonant form of the benzene ring against the other. This effect is related to the presence of a substituent angular group, the methoxy group in this case, with respect to the substitution axis. This effect is not so clear from the B structures. However, if we compare the same ring C-C distances in both A and B conformers, the changes due to the orientation of the methoxy group

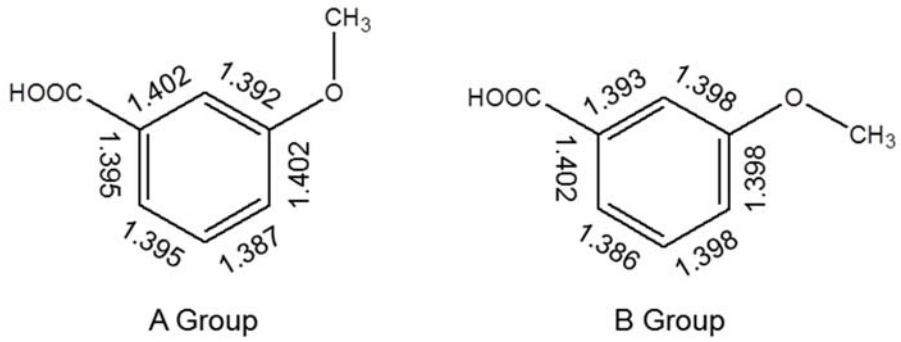


**Figure 3.** Schematic representation of the AGIBA effect in *m*-anisic acid (*m*-AA), which shows the prevalent canonical resonant form of the benzene ring for A and B groups of the monomer. All the bond distances predicted at B3LYP-D3/6-311++G(d,p) level of theory are given in Å.

become evident. This behavior was also observed for the anisole molecule[36] but not in the *o*-AA,[25] which has the same substituents as *m*-AA in an *ortho* disposition. The comparison of the $r_e$ parameters of the four detected *m*-AA forms with those corresponding to the *m*-AA – FA conformers (see Tables S2 and S3) indicates that the ring structure does not seem to be altered by the *m*-AA – FA interaction. This corroborates that the acid group does not have a net influence on the ring structure. Instead, the interaction with FA does affect to the structure of the *m*-AA COOH group as could be expected if the effects of RAHB[5] are taken into account. These effects can be further verified by comparison of the predicted structures of bare and bounded FA (see Tables S2 and S3). Moreover, it is interesting to remark that the distance $O_{AA}$-H$\cdots O_{FA}$ is predicted to be shorter than the $O_{AA}\cdots$H-$O_{FA}$ length in all the conformers observed.

The minimum energy pathways along the PES for interconversion between the observed conformers were also investigated. Two different dihedral angles $\angle C_2$-$C_1$-$C_7$-$O_9$ and $\angle C_2$-$C_3$-$O_8$-$C_{11}$ (see Figure 1) govern the interconversion pathways. The dihedral angle $\angle C_2$-$C_1$-$C_7$-$O_9$ is associated to the C-COOH torsion and relates forms 1 and 2. The dihedral angle $\angle C_2$-$C_3$-$O_8$-$C_{11}$ is in turn associated to the C-$OCH_3$ methoxy group torsion and describes the interconversion between the A and B conformers. The corresponding potential energy functions shown in Figures S4 and S5 were predicted at the MP2/aug-cc-pVDZ level of theory, because this level was found reliable to describe the interconversion between the two *cis* forms observed in *o*-AA.[25] The calculated energy barriers for the C-COOH and C-$OCH_3$ torsions were respectively 2400 $cm^{-1}$ and 1200 $cm^{-1}$. The same explorations were done for the interconversion between the four observed conformers of the *m*-AA – FA complex. These potential energy functions are also included in the supporting information as Figures S6 and S7. The calculated energy barriers have the same values as in the monomer, indicating that the interaction with FA does not affect to the

C–$OCH_3$ torsion potential energy function and only affect slightly to the C–COOH torsional motion.

**Relative abundances**

Relative intensity measurements of the same sets of $\mu_a$-type transitions for the monomer and for the complex conformers were done in the CP-FTMW spectra (see Figure 2). The intensities can be related to the relative populations in the jet by assuming that the cooling in the supersonic expansion brings all the molecular systems to the ground vibrational state of each observed conformation.[41] The intensities of the $\mu_a$-type lines of conformer *i*, with a value of the dipole moment component given by $(\mu_a)_i$ and with number density $N_i$ in the jet, have been assumed to be proportional to $(\mu_a)_i^2 N_i$. Using the predicted values of $\mu_a$ (see Table 1), the estimated relative abundance ratios are $N_{A1}/N_{A2}/N_{B2}/N_{B1}$=100/49(10)/13(4)/7(1) for the monomer conformers and $N_{A1\text{-}F1}/N_{A2\text{-}F1}/N_{B2\text{-}F1}/N_{B1\text{-}F1}$=100/52(11)/13(1)/9(2) for the cluster forms. The intensity of the cluster transitions is much lower than that for the monomer lines (see Figures 2 and S3). These abundance ratios, which correspond to the experiments done with Ar, do not change substantially when using other carrier gases. The relative intensity values thus show that A1 form is the most populated conformation in the expansion, despite the fact that it has the lowest intensity transitions. Moreover, the relative populations of the complex conformers are roughly the same as those of the corresponding monomer conformers.

The populations predicted using the Gibbs energies (Table 1), calculated from the harmonic frequencies, at the B3LYP-D3/6-311++G(d,p) level of theory, are $N_{A1}/N_{A2}/N_{B2}/N_{B1}$=100/76/45/41 for the monomer forms and $N_{A1\text{-}F1}/N_{A2\text{-}F1}/N_{B2\text{-}F1}/N_{B1\text{-}F1}$=100/100/57/51 for the cluster conformers. Complementary relative abundances predictions at

the MP2/aug-cc-pVDZ level of theory show $N_{A1}/N_{A2}/N_{B2}/N_{B1}$=100/74/42/40 for the monomer forms and $N_{A1\text{-}F1}/N_{A2\text{-}F1}/N_{B2\text{-}F1}/N_{B1\text{-}F1}$=100/88/45/46 for the cluster conformers. Their comparison to the experimental ones will be addressed below.

The experimental relative intensities indicate that the relative abundance of the different *m*-AA conformers is the same as that for the corresponding *m*-AA – FA complex forms. This is consistent with the hypothesis of a kinetic mechanism for complex formation in the first stages of the expansion. Assuming a high enough concentration of FA, the complex concentration would depend on the relative abundances of the *m*-AA conformers. Once the complexes are seeded in the expansion stream, the evolution to equilibrium is quenched and the initial relative abundances are preserved as the expansion cools down all species in the jet. Similar observations for related systems as *o*-AA-water[25] or *o*-AA-FA complexes[21] corroborate this mechanism for complex formation in the supersonic jet.

It is interesting to compare the population ratio between the A and B conformers. The theoretical calculations predict this ratio to be A:B ≈ 2:1 for either the monomer or the cluster. In previous studies done in solution[23] this ratio was reported to be 3:1. In the present work done in a supersonic expansion the experimental ratio is 7:1, more than two or three times higher than the values in solution or theoretical, respectively. Despite the differences, the conformer abundance ordering is the same in all cases. These discrepancies might indicate the existence of B→A conformational collisional relaxation in the jet,[42] but no substantial intensity changes were observed when using different carrier gases. On the other hand, the exploration of the PES surfaces for the C-COOH and C-$OCH_3$ torsions (see figures S4-S7) predict barriers that seem to be high enough to preclude such collisional relaxation.

In order to explain the preferred stabilization of forms A, steric interactions[43] between the methoxy and the carboxylic groups should be discarded. The stabilization of the A species might be explained if the interaction between the local electric dipole moments of each functional group is taken into account. While the relative dipole moments of the carboxylic and methoxy groups are nearly parallel in A conformers, in B conformers, they are disposed in a quasi-perpendicular disposition, making it less convenient to keep a stable dipole-dipole interaction.

**Dissociation energies**

The intermolecular stretching vibration is approximately coincident with the *a* inertial axis in all the four *m*-AA – FA conformers. This allows estimation of the stretching force constant from the centrifugal distortion constant $\Delta_J$, using the pseudo diatomic approximation.[44] The dissociation energy can be then estimated by assuming a Lennard-Jones potential function for this motion.[45] These experimental estimations of the dissociation energies are compared in Table 4 with the theoretical BSSE[33] corrected values. This approximated approach gives equal dissociation energies for all four *m*-AA – FA conformers within the uncertainties associated with the experimental centrifugal distortion constants. The equality of the dissociation energies can be expected since all four *m*-AA – FA conformers show the same acid-acid interaction, despite their differences in the configuration of *m*-AA. As shown in Table 4, the dissociation energy values are comparable to those observed for clusters having the same double hydrogen bond interaction as the four conformers of the *m*-AA cluster: benzoic acid – FA,[15] difluoroacetic acid – FA,[20] acrylic acid – FA[18] or the forms of *o*-AA – FA with *o*-AA in the *cis*-COOH arrangement.[21]

**Table 4**. Dissociation energies ($E_D$) (in kJ mol$^{-1}$) estimated from the pseudo diatomic approximation ($E_D$ (exp)) and predicted using the counterpoise procedure at the MP2/6311++G(d,p) ($E_D$(MP2)) and B3LYP-D3/6311++G(d,p) ($E_D$(B3LYP)) levels of theory for the *m*-anisic aid – formic acid dimers (*m*-AA – FA). Dissociation energies are compared to those of related acids - FA clusters.

| | $R_{CM}$ / Å [a] | $E_D$ (exp) | $E_D$ (MP2) | $E_D$ (B3LYP) |
|---|---|---|---|---|
| ***m*-AA-FA A1-F1** | 5.5663 | 51(7) [b] | 61.0 | 89.0 |
| ***m*-AA-FA A2-F2** | 5.6332 | 63(9) | 61.9 | 90.3 |
| ***m*-AA-FA B2-F1** | 5.7786 | 72(13) | 61.2 | 88.9 |
| ***m*-AA-FA B1-F1** | 5.7281 | 85(17) | 61.4 | 90.1 |
| ***o*-AA-FA T1-F-1** [c] | 4.7763 | 30(2) | 40.4 | 53.1 |
| ***o*-AA-FA T1-F-2** | 5.1301 | 7.1(4) | 37.4 | 52.3 |
| ***o*-AA-FA C2-F-1** | 5.2516 | 76(8) | 63.5 | 86.0 |
| ***o*-AA-FA C1-F-1** | 5.1875 | 62(5) | 64.5 | 86.8 |
| **DFAA-FA *trans*** [d] | | 61.7 | 49.0 | - |
| **DFAA-FA *gauche*** | | 63.3 | 50.5 | - |
| **AA-FA *cis*** [e] | | 64 | 51 | - |
| **AA-FA *trans*** | | 64 | 52 | - |
| **BA-FA**[f] | | - | 51.4 | - |

[a] $R_{CM}$ is the distance between the center of mass of each subunit, determined from $r_e$ structure. [b] Standard error is given in parentheses in units of the last digits. It was derived from the standard error of $\Delta_J$ constant. [c] *o*-Anisic acid – formic acid cluster, reference 21. [d] Difluoroacetic acid – formic acid cluster, reference 20. [e] Acrylic acid – formic acid cluster, reference 18. [f] Benzoic acid – formic acid cluster, reference 15.

**Comparison between *m*-anisic acid and the *o*- anisic acid isomers**

It is worth comparing the structure and properties obtained in this work on *m*-AA with those previously reported for *o*-AA.[25] The *ortho* isomer contains three conformers for which the structure is dominated by the intramolecular interactions between the carboxyl and methoxy groups. The most stable conformer of *o*-AA has a *trans*-COOH arrangement and an attractive O-H···O hydrogen bond intramolecular interaction between both functional groups. This hydrogen bond interaction fixes the orientation of the COOH and methoxy groups so that there is only one low energy form in the *trans* configuration in the carboxylic group. The other two conformers of *o*-AA have a *cis*-COOH arrangement with two possible orientations with respect to the methoxy group. For these two forms the structure is ruled by a repulsive steric O···O intramolecular interaction between the acid and methoxy groups. This interaction is so strong that it drives the torsion of the acid group, resulting in a loss of its co-planarity with the ring, which is favored by resonance. The methoxy group has only one possible arrangement since the steric $CH_3$···O repulsion hinders any conformation with the methyl group close to the acid group. In contrast, direct attractive or repulsive intramolecular interactions between the acid and methoxy groups are precluded in *m*-AA. Thus, in *m*-AA, the structure of all the observed conformers is governed by the resonance between the functional groups and the aromatic ring and probably by the electrostatic interactions between the local electric dipoles of both functional groups. The resonant effect stabilizes all the forms into planar skeleton structures.

The structural differences should be at the origin of the different chemical reactivity and properties of *o*- and *m*-AA isomers. The rotational spectrum of *o*-AA, studied with the same techniques used here, contains rotational lines of other structurally similar molecules like salicylic acid, methyl salicylate or methyl 2-methoxybenzoate.[25] These systems can be the result

of recombination reactions that exchange the $CH_3$ and an H atom reaction upon heating of *o*-AA. These reactions could be explained by invoking inter- or intra-molecular acid catalysis that is possible by the interactions between the acid and methoxy group. The spectrum of *m*-AA obtained under the same condition does not show lines of any potential reaction products.

In addition, the structural differences between *o*- and *m*-AA are also expected to have consequences in the thermodynamics of both systems. The intramolecular hydrogen bond and the lower number of conformers in *o*-AA compared to *m*-AA indicated a smaller number of states accessible in the former and thus to a higher entropy in *m*-AA.

The forces dominating the structure in both *o*- and *m*-AAs seem to prevail also in their complexes. In *o*-AA two conformers have been observed in a supersonic expansion for the complexes with water,[25] and four for the complexes with FA.[21] In both cases, the structures and particular features of the monomer conformers are preserved upon complexation. In fact, *o*-AA constitutes the first case in which complexes of a *trans*-COOH arrangement with water or FA were observed and were the most abundant species detected in the supersonic expansion. The *o*-AA – water[25] and *o*-AA – FA[21] *cis*-COOH complexes keep practically the same non-planar configurations as in the *o*-AA monomer. Therefore, the structure of *o*-AA – water[25] and *o*-AA – FA[2119] clusters is dominated by the same intramolecular interactions between the methoxy and the carboxylic groups that control the *o*-AA monomer structure. In the case of *m*-AA – FA complex the same happens and the four conformers observed are planar and thus mainly stabilized by resonance.

## CONCLUSIONS

Four different conformers of *m*-AA have been detected in a supersonic jet and characterized by rotational spectroscopy. These conformers, labelled as A1, A2, B1 and B2 (see Figure 1), reflect the combination of the four possible orientations of the methoxy (A-B) and acid (1-2) groups. This gas phase detection contrasts with the observations in solution, where only the disposition of the methoxy group (A or B) could be identified.[23] In the presence of FA, the spectra of four heterodimer conformers that preserve the structure of the *m*-AA forms have been detected. In all cases *m*-AA interacts with FA forming the same sequential cycle through a double O-H···O hydrogen bond. The observed planar moment $P_{cc}$ show that all the identified species have a planar skeleton with all the heavy atoms lying in the *ab* plane. The intensity analyses show that the relative abundances of the four *m*-AA conformers are the same as those found for the corresponding *m*-AA – FA complex forms. This proves the hypothesis that a kinetic mechanism dominates the complex formation, which takes place in the first steps of the supersonic expansion where the complex abundances depend on the populations of the monomer forms. The population rate observed for the A:B species in the *m*-AA monomer and in the *m*-AA – FA complex are of *ca.* 7:1, higher than the predicted ratio of 2:1 and the solution ratio of 3:1.[23] This might indicate the existence of relaxation processes in the jet although no intensity changes were observed in the experiments done with different carrier gases. Despite the differences indicated above, the conformer abundance ordering is consistent in all cases. The dissociation energies demonstrate that all the complex conformations have the same stabilization energies as could be expected from their hydrogen bonding structures.

## ASSOCIATED CONTENT

**Supporting Information**. (a) Completion of reference 34 (a) Tables and Figures of the predicted stable conformations of the *m*-AA – FA heterodimer; (b) Figures of the observed spectra; (c) Tables of transition frequencies. This material is available free of charge via Internet at.

## AUTHOR INFORMATION

Corresponding Authors:

sblanco@qf.uva.es (SB)

jclopez@qf.uva.es (JCL)

ORCID

Alberto Macario: 0000-0002-1196-3844. Susana Blanco: 0000-0002-1196-3844. Javix Thomas 0000-0002-0210-7982. Yunjie Xu 0000-0003-3736-3190. Juan Carlos López: 0000-0003-1028-779X

Notes

The authors declare no competing financial interest.

## ACKNOWLEDGMENT

AM, SB and JCL acknowledge the Ministerio de Economía y Competitividad (Grant CTQ2016-75253-P) for financial support. AM acknowledges the University of Valladolid for the Ph. D. grant (Contratos Predoctorales UVa) and the mobility grant (Ayudas para estancias breves en el desarrollo de tesís doctorales UVa) and YX for her kind hospitality. The research in Edmonton was funded by the University of Alberta and the Natural Sciences and Engineering

Research Council (NSERC) of Canada. YX acknowledges access to the computing facilities of the Shared Hierarchical Academic Research Computing Network (SHARCNET: www.sharcnet.ca), the Western Canada Research Grid (Westgrid) and Compute/Calcul Canada. YX is Tier I Canada Research Chair in Chirality and Chirality Recognition.

REFERENCES

(1) Kanchan, S.; Jayachandra, D. N. S. Effect of Parthenium Hysterophorus on Nitrogen-Fixing and Nitrifying Bacteria. *Can. J. Bot.* **1981**, 59, 199-202.

(2) Lynas, J. F.; Walker, B. Peptide Argininol "Inverse Substrates" of Anisic Acid: Novel Inhibitors of the Trypsin-Like Serine Proteinases. *Bioorg. Med. Chem. Lett.* **1997**, 7, 1133-1138.

(3) Maffei, M.; Bertea, C. M.; Garneri, F.; Scannerini, S. Effect of benzoic acid hydroxy- and methoxy- ring substituents during cucumber (Cucumis sativus L.) germination. I. Isocitrate liase and catalase activity. *Plant. Sci.* **1999**, 141, 139-147.

(4) Flavouring agent from FAO/WHO Food Additive Evaluations (JECFA). JECFA number: 882; FEMA number: 3944.

(5) Gilli, G.; Belluci, F.; Ferretti, V.; Bertolasi, V. Evidence for Resonance-Assisted Hydrogen Bonding from crystal-structure correlations on the enol form of the $\beta$-diketone fragment. *J. Am. Chem. Soc.* **1989**, 111, 1023-1028.

(6) Francis, B. R.; Watkins, W.; Kubelka, J. Double hydrogen bonding between side chain carboxyl groups in aqueous solutions of poly (*β*-L-Malic Acid): implication for the evolutionary origin of nuclei acids. *Life* **2017**, 7, 35.

(7) Feng, G.; Gou, Q.; Evangelisti, L.; Caminati, W. Frontiers in rotational Spectroscopy: Shapes and tunneling dynamics of the four conformers of the acrylic acid-difluoroacetic acid adduct. *Angew. Chem. Int. Ed.* **2014**, 53, 530-534.

(8) Daly, A. M.; Douglass, K. O.; Sarkozy, L. C.; Neill, J. L.; Muckle, M. T.; Zaleski, D. P.; Pate, B. H.; Kukolich, S. G. Microwave measurements of proton tunneling and structural parameters for the propiolic acid-formic acid dimer. *J. Chem. Phys.* **2011**, 135, 154304.

(9) Löwdin, P. O. Quantum genetics and the aperiodic solid. Some aspects on the biological problems of heredity, mutations, ageing, and tumors in view of the quantum theory of the DNA molecule. *Adv. Quantum Chem.* **1965**, 2, 213-360.

(10) Catalán, J.; Kasha, M. Photophysics of 7-azaindole, its doubly-H-bounded base-pair, and corresponding proton-transfer-tautomer dimeric species, via defining experimental and theoretical results. *J. Phys. Chem. A* **2000**, 104, 10812-10820.

(11) Costain, C. C.; Srivastava, G. P. Study of hydrogen bonding. The microwave rotation spectrum of $CF_3COOH$-HCOOH. *J. Chem. Phys.* **1961**, 35, 1903-1904.

(12) Bellot, E. M.; Wilson Jr., E. B. Hydrogen bonded bimolecular complexes of carboxylic acids in the vapor phase: observation and characterization by low resolution microwave spectroscopy. *Tetrahedron* **1975**, 31, 2896-2898.

(13) Martinache, L.; Kresa, W.; Wegener, M.; Vonmont, U.; Bauder, A. Microwave spectra and partial substitution structure of carboxylic acid biomolecules. *Chem. Phys.* **1990**, 148, 129-140.

(14) Tayler, M. C. D.; Ouyang, B.; Howard, B. J. Unraveling the spectroscopy of coupled intramolecular tunneling modes: A study of double proton transfer in the formic-acetic acid complex. *J. Chem. Phys.* **2011**, 134, 054316.

(15) Evangelisti, L.; Écija, P.; Cocinero, E. J.; Castaño, F.; Lesarri, A.; Caminati, W.; Meyer, R. Proton tunneling in heterodimers of carboxylic acids: A rotational study of the benzoic acid-formic acid bimolecule. *J. Phys. Chem. Letts.* **2012**, 3, 3770-3775.

(16) Feng, G.; Favero, L. B.; Maris, A.; Vigorito, A.; Caminati, W.; Meyer, R. Proton transfer in homodimers of carboxylic acids: The rotational spectrum of the dimer of acrylic acid. *J. Am. Chem. Soc.* **2012**, 134, 19281-19286.

(17) Li, W.; Evangelisti, L.; Gou, L.; Caminati, W.; Meyer, R. Barrier to proton transfer in the dimer of formic acid: a pure rotational study. *Angew. Chem. Int. Ed.* **2019**, 131, 869-875.

(18) Feng, G.; Gou, Q.; Evangelisti, L.; Xia, Z.; Caminati, W. Conformational equilibria in carboxylic acid bimolecules: A rotational study of acrylic acid-formic acid. *Phys. Chem. Chem. Phys.* **2013**, 15, 2917-2922.

(19) Gou, Q.; Feng, G.; Evangelisti, L.; Caminati, W. Conformational equilibria in bimolecules of carboxylic acids: A rotational study of fluoroacetic acid-acrylic acid. *J. Phys. Chem. Letts.* **2013**, 4, 2838-2842.

(20) Gou, Q.; Feng, G.; Evangelisti, L.; Caminati, W. Conformers of dimers of carboxylic acids in the gas phase: A rotational study of difluoroacetic acid – formic acid. *Chem. Phys. Letts.* **2014**, 591, 301-305.

(21) Macario, A.; Blanco, S.; Thomas, J.; Xu, Y.; López, J. C. Competition between intra- and inter-molecular hydrogen bonding: *o*-anisic acid ⋯ formic acid heterodimer. Under submission.

(22) Kalinowska, M.; Swiderski, G.; Lewandowski, W. Effect of substituent position and lithium, sodium and potassium on the electronic structure of *o*-, *m*- and *p*-methoxibenzoic acids. *Polyhedron* **2009**, 28, 2206-2218.

(23) Exner, O.; Fiedler, P.; Budesínský, M. Conformation of Steric Effects in mono- and dimethoxybenzoic acids. *J. Org. Chem.* **1999**, 64, 3513-3518.

(24) Blanco, S.; Pinacho, P.; López, J. C. Hydrogen-bond cooperativity in formamide$_2$-water: a model for water-mediated interactions. *Angew. Chem. Inter. Ed.* **2016**, 55, 9331-9335.

(25) López, J. C.; Macario, A.; Blanco, S. Conformational equilibria in *o*-anisic acid and its monohydrated complex: the prevalence of the *trans*-COOH form. *Phys. Chem. Chem. Phys.* **2019**, 21, 6844-6850.

(26) Krygowski, T. M.; Wisiorowski, M.; Howard, S. T.; Stolarczyk, L. Z. Angular-Group-Induced Bond Alteration. I. Origin of the effect from *ab initio* calculations. *Tetrahedron* **1997**, 53, 13027-13036.

(27) Howard, S. T.; Krygowski, T. M.; Ciesielski, A.; Wisiorowski, M. Angular-Group-Induced Bond Alteration. II. The magnitude and the nature of the effect and its application to polynuclear benzenoid systems. *Tetrahedron* **1998**, 54, 3533-3548.

(28) Brown, G. G.; Dian, B. C.; Douglass, K. O.; Geyer, S. M.; Shipman, S. T.; Pate, B. H. A Broadband Fourier Transform Microwave Spectrometer Based on Chirped Pulse Excitation. *Rev. Sci. Instrum.* **2008**, 79 (5), 4–5.

(29) Thomas, J.; Yiu, J.; Rebling, J.; Jäger, W.; Xu, Y. Chirped-pulse and cavity-based Fourier transform microwave spectroscopy of a chiral epoxy ester: methyl glycidate. *J. Phys. Chem. A* **2013**, 117, 13249-13254.

(30) Pinacho, P.; Blanco, S.; López, J. C. The complete conformational panorama of formanilide-water complexes: the role of water as a conformational switch. *Phys. Chem. Chem. Phys.* **2019**, 21, 2177-2185.

(31) Xu, Y.; Jäger, W. Evidence for heavy atom large amplitude motions in RG-cyclopropane van der Waals complexes (RG=Ne, Ar, Kr) from rotation-tunneling spectroscopy. *J. Chem. Phys.* **1997**, 106, 7968-7980.

(32) Xu, Y.; Wijngaarden, J. V.; Jäger, W. Microwave spectroscopy of ternary and quaternary van der Waals clusters. *Int. Rev. Phys. Chem.* **2005**, 24, 301-338.

(33) Boys, S. F.; Bernardi, F. The calculations of small molecular interactions by the differences of separate total energies. Some procedures with reduced errors. *Mol. Phys.* **1970**, 19 553-566.

(34) M. J. Frisch et al., *Gaussian 09*, Revision D.01, Gaussian, Inc., Wallingford CT, 2016.

(35) Watson, J. K. G. Aspects of Quartic and Sextic Centrifugal Effects on Rotational Energy Levels. In: Vibrational spectra and structure a Series of Advances; During, J. R., Ed.; Elsevier: Amsterdam, 1997, Vol. 6, pp. 1-89.

(36) Desyatnyk, O.; Pszczólkowski, P.; Thorwirth, S.; Krywowski, T. M.; Kisiel, Z. The rotational spectra, electric dipole moments and molecular structures of anisole and benzaldehyde. *Phys. Chem. Chem. Phys.* **2005**, 7, 1708-0715.

(37) Winnewisser, M.; Winnewisser, B. P.; Stein, M.; Birk, M.; Wagner, G.; Winnewisser, G.; Yamada, K. M. T.; Belov, S. P.; Baskakov, O. I. Rotational spectra of *cis*-HCOOH, *trans*-HCOOH and *trans*-H$^{13}$COOH. *J. Mol. Spectrosc.* **2002**, 216, 259-265.

(38) Suenram, R. D.; Crum, P. M.; Douglass, K. O.; Pate, B. H. Conformational studies in formic acid oligomers. The Ohio State 59th International Symposium on Molecular Spectroscopy.

(39) Priem, D.; Ha, T.-K.; Bauder, A. Rotational spectra and structures of three hydrogen-bonded complexes between formic acid and water. *J. Chem. Phys.* **2000**, 113, 169-175.

(40) Ioannou, I. I.; Kuczkowski, R. L. Microwave spectrum and structure of the argon-formic acid Van der Waals complex. *J. Phys. Chem.* **1994**, 98, 2231-2235.

(41) Esbitt, A. S.; Wilson Jr., E. B. Relative intensity measurements in microwave spectroscopy. *Rev. Sci. Instrum.* **1963**, 34, 901-907.

(42) Ruoff, R. S.; Klots, T. D.; Emilsson, T.; Gutowsky, H. S. Relaxation of Conformers and Isomers in Seeded Supersonic Jets of Inert Gases. *J. Chem. Phys.* **1990**, *93* (5), 3142–3150.

(43) Decouzon, M.; Exner, O.; Gal, J.-F.; Maria, P.-C. Non-classical buttressing effect: gas-phase ionization of some methyl-substituted benzoic acids. *J. Chem. Soc., Perkin Trans. 2* **1996**, 475-479.

(44) Millen, D. J. Determination of stretching force constants of weakly bound dimers from centrifugal distortion constants. *Can. J. Chem.* **1985**, 63, 1477-1479.

(45) Novick, S. E.; Harris, S. J.; Janda, K. C.; Klemperer, W. Structure and bonding of KrClF: Intermolecular force fields in Van der Waals molecules. *Can. J. Phys.* **1975**, 53, 2007.

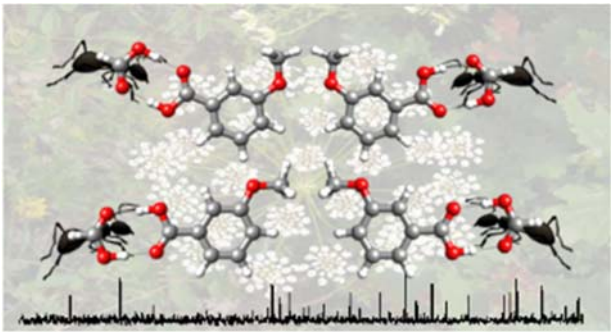

For Table of Contents Only